Finite Element Analysis applied to Electromagnetic Forces calculation on Power Transformers

L. H. Medeiros, G. Maschio, M. M. Oliveira, A. M. Kaminski, D. M. Bueno, V. C. Bender, T. B. Marchesan
Computer Aided Engineering Laboratory - INRI CAE
Federal University of Santa Maria - UFSM
Santa Maria, Brazil
leohm.29@gmail.coim

***Abstract*— High electromagnetic forces on power transformers windings may cause the equipment unavailability, resulting in technical and financial losses. To ensure its reliability, transformers must withstand the mechanical stresses demanded by the operation conditions. Once forces measurement and determination have a high degree of complexity, it is needed tools that support forces calculation and analysis accurately. This paper presents the Finite Element Analysis (FEA) applied to determine the electromagnetic forces and its distribution on transformer windings. A complete and close to the practice modeling is done, considering the magnetic core and lateral phases presence in a 3D and 3-phase configuration. The total, radial and axial forces over the windings, as well as its distribution around the core column and along its height are determined on the three phases. With precision and versatility, FEA may be widely applied by industry, contributing for more reliable transformers designs and in cost reduction.**

Keywords*— *Electromagnetic Forces, Finite Element Analysis, Power Transformers, Short-circuit, Transformer Design.

I. INTRODUCTION

Power transformers are used throughout the electrical system, regulating the voltage levels for different applications and ensuring the electrical energy transmission and supply. In addition to their technical importance for the system, transformers are the largest and the most expensive substation assets. Thus, their unavailability results in technical and financial losses, with the energy supply interruption and the repair or replacement of the equipment [1-3].

In order to avoid failures and ensure a safe operation, transformers designs must be robust and reliable, withstanding thermal, electrical and mechanical stresses when in operation. Some of failures that cause unavailability of transformers are due to the circulation of high currents in its windings, especially during short-circuit, resulting in large electromagnetic forces that can deform the windings and break up the dielectric insulation [3-5]. However, short-circuit tests to evaluate these forces are not trivial, due the high costs, and their determination is not simple, given the structure and measurements complexity [4]. As a result, several analytical methods to forces calculation and modeling through computer simulations have been proposed over the years to assist in transformer design.

Although widely used by industry, analytical equations in the literature use simplifications and approximations, and allow to determine only the total forces over windings, not their spatial distribution. In addition, equations resolution become more limited as the equipment geometry becomes more complex [6, 7]. Similarly, most of numerical simulations of power transformers also performs incomplete analysis or uses geometry simplifications, analyzing only specific cases, as ignoring the magnetic core presence, two dimensions (2D) or one-phase modeling [8-13].

Thereby, the Finite Element Analysis (FEA) is presented as a precise tool for calculate the electromagnetic forces and its distribution on transformer windings, within the Computer Aided Engineering concept. A complete three-phase transformer was modeled and simulated in a three dimensions (3D) configuration. During a short-circuit scenario, the radial and axial forces are determined and analyzed around the magnetic core column and along the windings height for three phases. The accurate results in comparison with the analytical equations from the literature used by industry, and the simulations versatility, makes FEA a great tool for more reliable transformers designs. In addition, FEA contributes to costs reduction with prototypes and tests by manufacturers.

II. ELECTROMAGNETIC FORCES ON TRANSFORMERS

The electromagnetic forces on transformers windings are result of the interaction between the current that circulates through them and the leakage magnetic flux in it are immersed. The force $\vec{F}$ (N/m³) is calculated through the Lorentz Law, according to (1), where $\vec{J}$ (A/m²) is the current density and $\vec{B}$ (T) is the magnetic flux density [3, 4, 7]

$$\vec{F} = \vec{J} \times \vec{B} \tag{1}$$

Due the curvature of leakage magnetic flux on top and bottom extremities of windings, it can be separated in radial and axial components. According to (1), the axial and radial components result in radial and axial forces, respectively. This paper analyzes only radial and axial forces on a concentric windings arrangement of same height. The analysis of this arrangement serves as a base for more complex arrangements. For same height concentric windings, the low voltage (LV) is considered the inner winding, while the high voltage (HV) the outer one.

Analyzing the radial forces, inner and outer windings suffer repulsion forces F_R, compressing the LV and expanding the HV. From the axial point of view, both the windings suffer axial compression forces F_A, leading to a maximum accumulated compression point in the middle of windings [3, 4, 7]. Fig. 1 illustrates the forces behavior for this arrangement.

https://doi.org/10.53316/sepoc2021.039

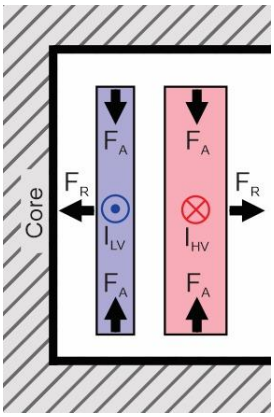

Fig. 1. Forces in concentric windings of same height.

High currents, as during short-circuit events, result in high electromagnetic forces, greater than the forces during the normal operation. The mechanical design must withstand these high forces, otherwise the windings deformations may cause several problems to the equipment, as the rupture of dielectric insulation, which results in intern short-circuits. These deformations may also lead to the increase of electrical stress inside the transformer, useful life reduction and overheating [3]. Thus, the electromagnetic forces calculation is extremely important to ensure the safe and correct operation of transformers.

III. Finite Element Modeling

For electromagnetic forces determination and analysis, a prototype transformer presented in [7] was modeled in a 3D and three-phase configuration, using the Ansys Electronics Desktop®. This complete modeling allows a more precise analysis, considering issues as the effect of magnetic core window and the adjacent phases presence. The constructive dimensions and electrical specifications are shown in Table I and Table II, respectively. To simplify the results understanding, the inner windings are called LV and the outer windings HV, even with the unitary transformation ratio, which do not interfere on electromagnetic forces theory.

The modeled transformer is shown in Fig. 2, with the LV and HV windings in blue and orange, respectively. The windings were modeled with 32 radial divisions around the core column, and with 20 axial divisions along its height. These divisions allow a more precise detailing of the distribution of radial and axial forces on the entire windings.

TABLE I. TRANSFORMER CONSTRUCTIVE DIMENSIONS

Three-phase Prototype – Constructive Dimensions	
Core window height	889 mm
Limbs distance	412.75 mm
Windings height - h	812.8 mm
Number of turns per winding	720
Core diameter - D_c	212.725 mm
Core height	1270 mm
Core steps	5
Windings thickness - $t_1 = t_2$	28.575 mm
Duct thickness - d_0	19.05 mm
Mean diameter of windings - D_m	307.975 mm
Mean diameter of inner winding - D_{m_in}	262.35 mm
Mean diameter of outer winding - D_{m_out}	357.6 mm

TABLE II. TRANSFORMER ELECRIC SPECIFICATIONS

Three-phase Prototype – Electric Specifications	
Nominal voltage	5.5 kV/5.5 kV
Nominal rating power	140 kVA
Nominal current	25.4 A
Impedance	4.24%
Peak asymmetrical 3-phase short-circuit current	1,527 A

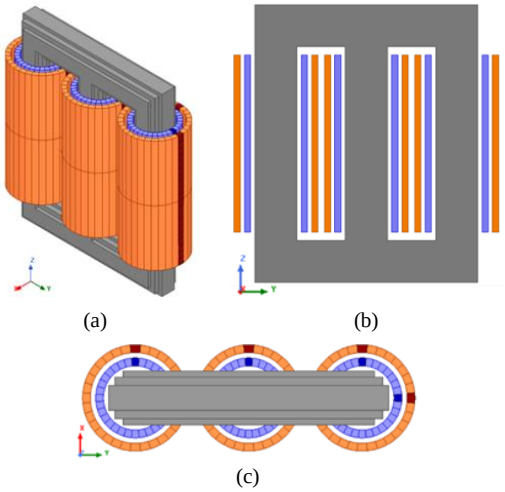

Fig. 2. Transformer modeling - (a) isometric view, (b) 2D section and (c) upper view.

A three-phase excitation was applied, with a peak asymmetrical 3-phase short-circuit current from Table II, representing the worst scenario with the highest forces. The simulation converged with about a 300 thousand elements mesh and a maximum energy error of 0.1%, during approximately 5 hours in a high performance computer.

IV. Results

From the modeling described in previous section and after the simulation convergence, the obtained results are analyzed. Table III presents the results for radial forces and axial compressions on the central phase of LV and HV windings, obtained with FEA and analytical equations discussed in [7], as well as the percentage difference among them. It is noted the good agreement of FEA, presenting a maximum difference about 7% between all the analyzed parameters.

TABLE III. COMPARISON BETWEEN FEA AND ANALYTICAL

Parameter	**FEA (kN)**	**Analytical (kN)**	**Difference (%)**
Radial HV	953.6415	1,029.454	7.364
Radial LV	749.866	755.25	0.712
Compression HV	13.969	13.853	-0.842
Compression LV	26.302	27.70	5.067
Total Compression	40.271	41.559	3.095

Once verified the good agreement of FEA results, the total radial and axial compression forces on three phases are presented in Table IV. It is noted that the total radial and compression forces present close values between central (Phase B) and lateral phases (Phases A and C). The small differences are analyzed in the sequence, detailing the forces distribution over the windings.

TABLE IV. FORCES COMPARISON BETWEEN THREE PHASES

Parameter	Phase A (kN)	Phase B (kN)	Phase C (kN)
Radial HV	947.122	953.6415	947.158
Radial LV	747.244	749.866	747.264
Compression HV	10.753	13.969	10.671
Compression LV	30.669	26.302	30.733
Total Compression	41.423	40.271	41.405

To support the forces distribution understanding, Fig. 3 and Fig. 4 illustrate the leakage magnetic flux and its vector lines behavior, respectively, a visual tool that analytical equations and simplified simulations does not allow. It is noted that the highest leakage flux concentration occurs in the region between inner and outer windings, and the lines curvatures on the top and bottom extremities, that can be better visualized in Fig. 5.

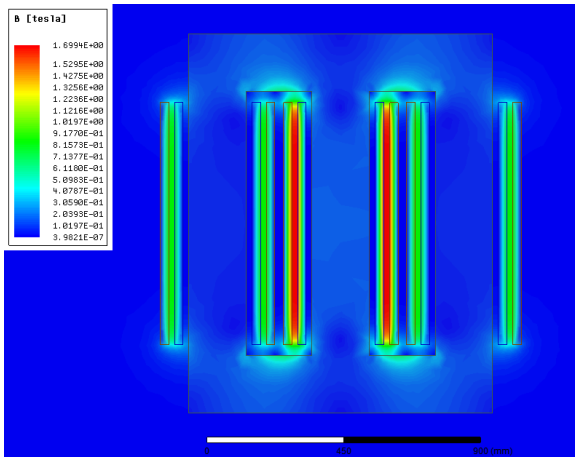

Fig. 3. Leakage magnetic flux density – 2D section.

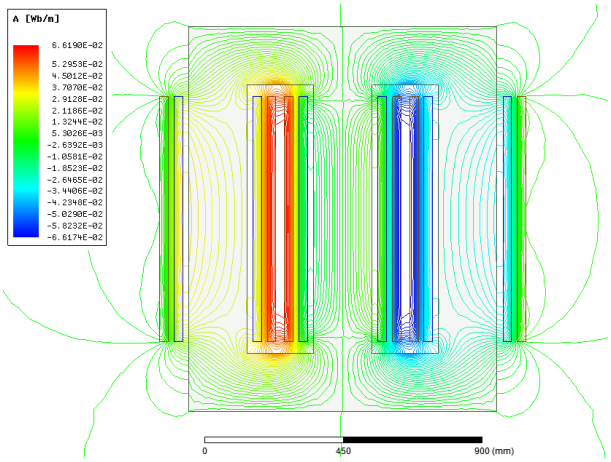

Fig. 4. Leakage magnetic flux vector lines – 2D section.

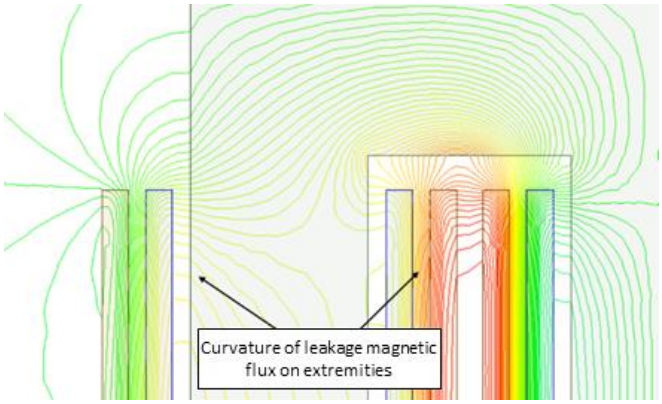

Fig. 5. Detail of leakage flux curvature on extremities.

From leakage magnetic flux behavior, Fig. 6 illustrates the electromagnetic forces vectors along the winding. It is observed that in the windings central region, where the leakage flux presents a rectilinear behavior, there are the predominance of repulsion radial forces only. On the other hand, in the top and bottom extremities, where the leakage flux presents curvatures, there are axial forces, tending to compress the winding.

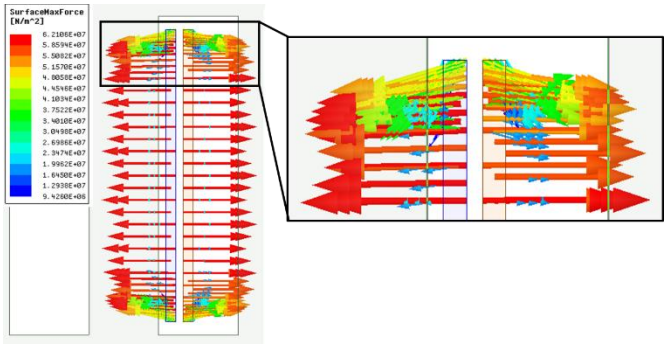

Fig. 6. Electromagnetic forces vectors.

The total radial and axial forces from Table IV are analyzed in a distributed form, separately, around the core column and along the windings.

A. Radial Forces Distribution

Analyzing the radial forces obtained in each one of the 32 modeled radial divisions, the behavior around the core column is observed, as illustrated in Fig. 7. The black dotted rectangle represents the magnetic core window seen from above, indicating the windings regions that are inside and outside it.

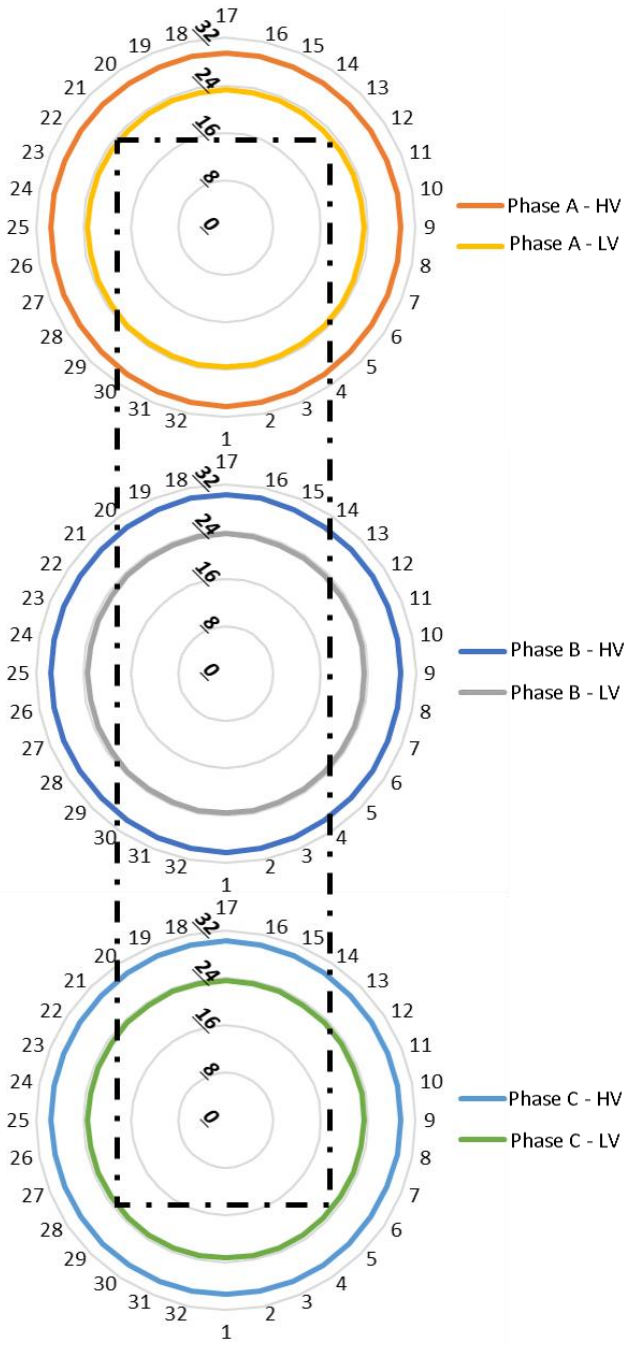

Fig. 7. Radial forces distributed radially around the core column (in kN).

It is noted that the radial forces are more intense on the outer windings, as already seen in Table IV, and present a homogeneity around the entire winding, with the same magnitude on the three phases, about 23 kN on the inner and 30 kN on the outer winding. This homogeneity indicates that the magnetic core window does not influence the radial forces magnitude, once the winding portion inside the window has the same force that the outside portion.

Through the modeled axial divisions, the radial forces behavior along the windings height is observed. Fig. 8 illustrates the radial forces distribution along the LV and HV windings height on the central phase (Phase B). Once central and lateral phases have the same behavior, the results on central phase are the same on the lateral ones. It is noted a greater magnitude in the central region, about 1.2 kN and 1.6 kN, with a decrease in top and bottom extremities regions, about 0.9 kN and 1.15 kN, on the LV and HV windings, respectively. It is also observed the constant behavior in the central region, due the rectilinear and uniform behavior of leakage flux there. This same behavior was already seen in vectors forces in Fig. 6.

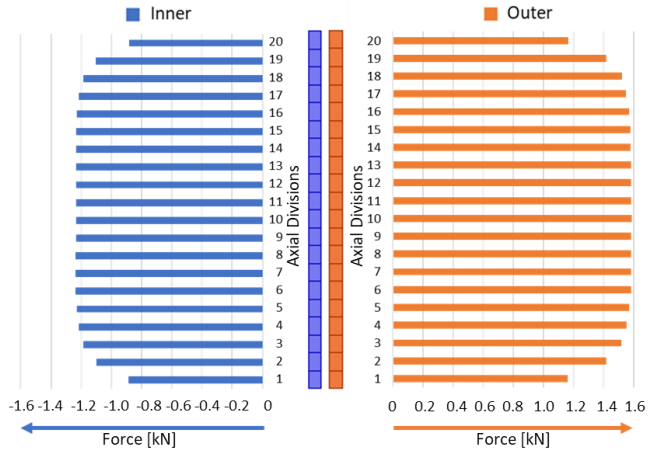

Fig. 8. Radial forces distributed axially along the winding height.

B. *Axial Forces Distribution*

Similarly, Fig. 9 illustrates the axial forces distribution on windings around the core column. Contrasting from radial forces, it is observed distinct behaviors for the portions inside and outside core window. The inner winding presents greater magnitude outside the window, 1.1 kN against 0.65 kN inside. The outer windings present an inverse behavior, with greater forces inside the window, 0.65 kN against 0.3 kN outside.

This behavior explains the values seen in Table IV. Once the Phase B has a bigger portion inside the window than the lateral phases A and C, it suffers a greater axial compression on the HV outer winding. Likewise, Phase B presents a lower axial compression on the LV inner winding than the lateral phases.

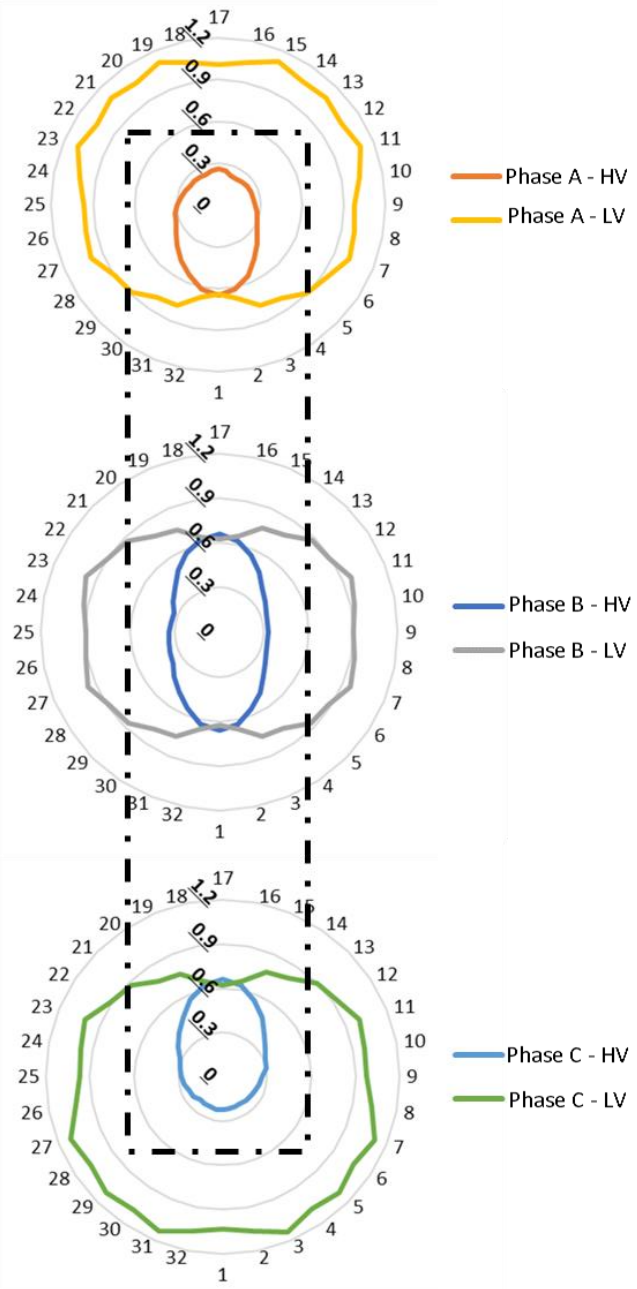

Fig. 9. Axial forces distributed radially around the core column (in kN).

This analysis shows that the presence of magnetic core window influences in axial forces magnitude and distribution around core column. Thereby, Fig. 10 illustrates the axial compression forces distributed axially, along the windings height, inside and outside the window. It is observed that in central region the axial forces tend to be null, acting only in the top and bottom extremities regions. This distribution leads to the compression of the winding, corroborating, once again, the vectors behavior from Fig. 6. Comparing inside and outside the window, as already mentioned, the inner windings present more intense axial forces on its outside, whereas the outer windings on its inside. This difference in relation to the core window leads to different maximum compressions on the regions inside and outside the window.

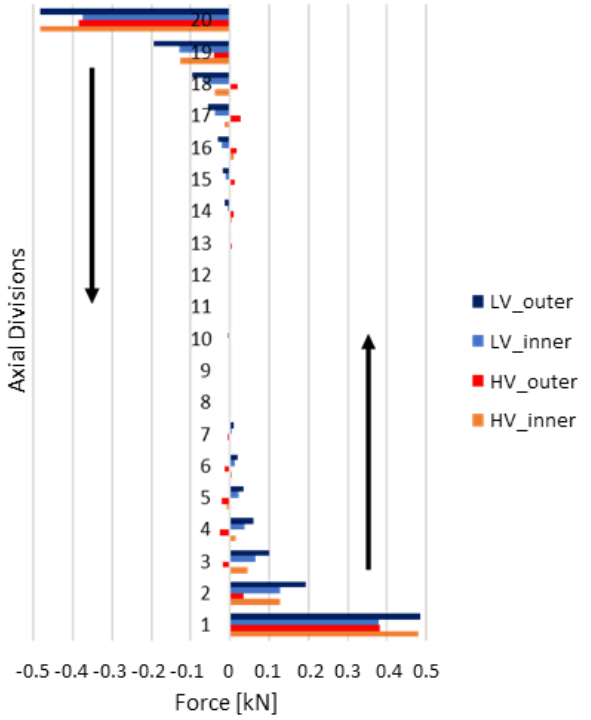

Fig. 10. Axial forces distributed axially along the winding height.

The Fig. 11 illustrates the accumulated axial compression along the windings height, on the 20 axial divisions modeled. It is noted that the compression inside the window is closer for inner and outer windings, about 0.65 kN. On the other hand, outside the window the compression on HV outer windings is lower and on LV inner windings is greater, about 0.3 kN and 0.9 kN, respectively.

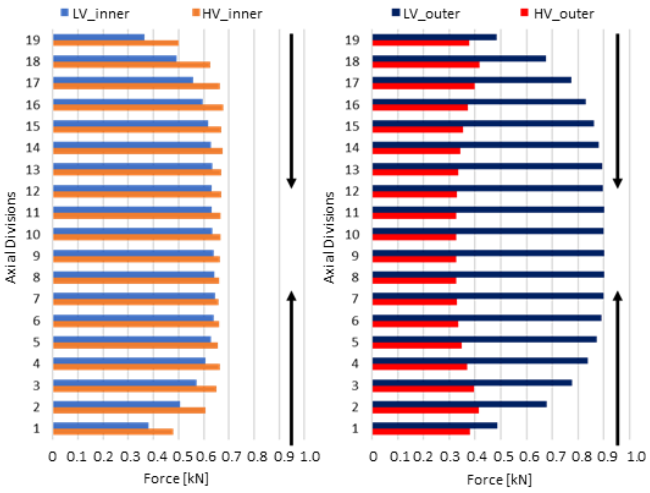

Fig. 11. Accumulated axial compression distributed axially along the winding height.

These magnitude differences on windings, due the constructive arrangement, mainly because of the winding position in relation to magnetic core, cannot be observed through analytical equations. As seen on Table III, the equation returns only the value of total force. The forces differences and distribution also cannot be visualized with simplified simulations, in only two dimensions, in an one-phase configuration or without the magnetic core window representation.

V. Conclusions

The electromagnetic forces on power transformers windings may cause equipment failures and interrupt the electric energy supply, mainly during short-circuits with high magnitude currents. Thus, the mechanical structure must be correctly calculated from the forces determination during the design stage. However, the determination of forces is not trivial, justifying the search for more precise tools and methods of calculation and analysis.

This paper presented a FEA of a concentric windings arrangement of same height, of a three-phase transformer. From the modeling performed, it was possible to calculate with precision the total radial and axial forces on the windings, as well as its distributions. With a modeling close to the practice, it was observed different behaviors over the windings, mainly due the magnetic core window presence. Comprehend the forces distribution is important to identify points of bigger or lower mechanical stresses, contributing to avoid over and undersized designs and helping in the material choices.

Thereby, simulations for FEA are shown a good tool to be applied by transformers industry during the design stage, contributing to the manufacturing of more reliable and economic equipment. Due the FEA versatility, its use reduces the prototype manufacturing and tests costs. The FEA also can be applied to investigate failure cases during operation. In addition to this, FEA can be performed to different winding arrangement and different operation conditions, not only short-circuit, as nominal and inrush conditions.

Acknowledgment

This study was financed in part by the Coordenação de Aperfeiçoamento de Pessoal de Nível Superior - Brasil (CAPES/PROEX) – Finance Code 001. The authors also would like to thanks the technical and financial support of Conselho Nacional de Desenvolvimento Científico e Tecnológico (CNPq), Universidade Federal de Santa Maria (UFSM), Programa de Pós-Graduação em Engenharia Elétrica (PPGEE) da UFSM and Instituto Nacional de Ciência e Tecnologia em Geração Distribuída (INCT-GD).

References

[1] A. D. Ashkezari, H. Ma and T. K. Saha, C. Ekanayake, “Application of Fuzzy Support Vector Machine for Determining the Health Index of the Insulation System of In-Service Power Transformers,” IEEE Trans. Dielec. Elec. Insul., vol. 20, no. 3, pp. 965-973, Jun. 2013.

[2] A. Jahromi, R. Piercy, S. Cress, J. R. R. Service and W. Fan, “An Approach to Power Transformer Asset Management Using Health Index,” IEEE Elec. Insul. Mag., vol. 25, no. 2, pp. 20-34, Mar. 2009.

[3] S. V. Kulkarni and S. A. Khaparde, Transformer Engineering: Design and Practice. New York: Marcel Dekker, 2004.

[4] R. M. Del Vecchio, B. Poulin, P. T. Feghali, D. M. Shah and R. Ahuja, Transformer Design Principles: With Application to Core-form Power Transformers. CRC Press, 2002.

[5] IEC Ability to withstand short-circuit, IEC 600076, Part 5, 2000.

[6] E. Billig, “Mechanical stresses in transformer windings,” Journal Inst. Elec. Eng., vol. 93, no. 33, pp. 227-243, Jun. 1946.

[7] M. Waters, The Short-Circuit Strength of Power Transformers. London, England: Macdonald & Co., 1966.

[8] A. Bakshi and S. V. Kulkarni, “Analysis of Buckling Strength of Inner Windings in Transformers Under Radial Short-Circuit Forces,” IEEE Trans. Power Del., vol. 29, no. 1, pp. 241-245, Feb. 2014.

[9] B. Zhang, N. Yan, S. Ma and H. Wang, "Buckling Strength Analysis of Transformer Windings Based on Electromagnetic Thermal Structural Coupling Method," IEEE Trans. Appl. Supercond., vol. 29, no. 2, pp. 1-4, Mar. 2019.

[10] S. L. Ho, Y. Li, H. C. Wong, S. H. Wang and R. Y. Tang, "Numerical simulation of transient force and eddy current loss in a 720-MVA power transformer," IEEE Trans. Mag., vol. 40, no. 2, pp. 687-690, Mar. 2004.

[11] H. Zhang, B. Yang, W. Xu, S. Wang, G. Wang, Y. Huangfu and J. Zhang, "Dynamic Deformation analysis of Power Transformer Windings in Short-Circuit Fault by FEM," IEEE Trans. Appl. Supercond., vol. 24, no. 3, pp. 1-4, Jun. 2014.

[12] M. Steures and K. Frölich, “The Impact of Inrush Currents on the Mechanical Stress of high Voltage Power Transformer Coils,” IEEE Trans. Power Del., vol. 17, no. 1, pp. 155-160, Aug. 2002.

[13] J. Faiz, B. M. Ebrahimi and T. Noori, "Three- and Two-Dimensional Finite-Element Computation of Inrush Current and Short-Circuit Electromagnetic Forces on Windings of a Three-Phase Core-Type Power Transformer," IEEE Trans. Mag., vol. 44, no. 5, pp. 590-597, May. 2008.